Structures in a Supersonic Plane Jet due to Symmetric/Antisymmetric Unstable Modes at High Mach Numbers

Daisuke WATANABE* and Hiroshi MAEKAWA*
* The University of Electro-Communications,Chofu-shi,Tokyo 182-8585, Japan

This paper describes an analytical and numerical investigation of plane supersonic jet. Results of linear stability analyses for Mc=0.38 to Mc=1.51 show that the dominant mode depends upon the Mach numbers. For Mach number less than 1.5 the most unstable mode is antisymmetric. For Mc over 1.5, the dominant mode is symmetric. 2-D spatially developing direct numerical simulations for Mc=1.51 show that the dilatation formed around the jet center plane is very strong, however, weak outside. It is confirmed by 3-D temporal DNS for Mc=1.13 that the structure of the flow field depends on the initial conditions, because the linear growth rates of the 2-D symmetric and 3-D antisymmetric mode are comparatively similar.

Key Words: Compressible flow, Plane supersonic jet, DNS, linear stability analysis

1. Introduction

A fundamental problem in the study of compressible shear flows is the analysis of compressible jets, which can be found in such diverse contexts as rocket, scramjet, ramjet, turbofan and turbojet engines. Recently and with the new noise regulations, reducing jet engines acoustic emissions became a major challenge for aircraft designers and manufacturers (see Lele[1],Colonius[2],Mitchell[3] et al.). The understanding of the effect of jet structures on the noise generation (acoustic waves) is very crucial for noise control. Therefore and in this challenging context, we investigated the linear stability of high Mach number plane jets, then, and by means of DNS, the development of the corresponding supersonic flow structures after being perturbed with the unstable modes.

2. Computational Details

For stability analysis, the linear stability equations of compressible viscous jet were solved using a direct spectral method. We assumed that the disturbances are in the form of normal modes.

For direct numerical simulations, sixth-order compact finite difference schemes[4] were used in all directions. Time advancement was performed by fourth-order Runge-Kutta algorithm. For 2-D spatial case, the computational mesh was $N_x \times N_y = 600 \times 300$ and for 3-D temporal case, the computational mesh was $N_x \times N_y \times N_z = 100 \times 200 \times 100$.

3. Results

3.1. 2-D Results

3.1.1. linear stability

Fig.1 is the results of linear stability analysis when $\beta = 0$ ($\theta = tan^{-1}(\beta/\alpha)$) for Re=1000 and Mc less than 0.75. (Mc stands for convective Mach number) Horizontal and vertical axes are wave number α and linear growth rate ω_i respectively. The curve plotted the eigenvalue of largest growth rate for each α. Continuous line, dashed line, and dotted line represent results of Mc=0.38, Mc=0.57 and Mc=0.75 respectively. Bold line corresponds to antisymmetric mode (hereafter referred to as A1) and fine line corresponds to symmetric mode (hereafter referred to as S1). For convective Mach number less than 0.75, two unstable modes A1 and S1 exist, but in this range, the antisymmetric mode is dominant. With the increase of Mc, the growth rates of these modes decrease, however the growth rate of the S1 decreases quicker than A1. In Mc=0.85, there is no positive growth rate of S1 mode. Fig.2 corresponds to higher Mach number case. In this Mach number range, unstable modes, other than A1, show the largest growth rate at higher wave numbers. In Mc=1.51, five antisymmetric and symmetric modes appeared alternatively, therefore we called them A1, S2, A2, S3, A3 respectively. S2 mode which appears first by the increase in Mc is symmetrical, and this mode becomes dominant over Mc=1.13. Kudryavtsev[5] performed spatial 2-D DNS of Mc=1.5 plane jet that can be considered as a validation to our findings. From the analysis of the eigenfunction, it was proven that S2 mode differed from the S1 mode.

Pressure eigenfunctions at Mc=1.51 (only S1 mode corresponds to Mc=0.57) are shown in Fig.3. In this figure, the maximum magunitudes of the S1 mode eigenfunction is located in both sides of jet center and S2 mode eigenfunction is located at jet center and the both sides, which implies that S2 is different from

S1. Besides the number of eigenfunction's maximal magunitudes of A1 and S1 which have 2 peaks, S2, A2, S3 and A3 have 3, 4, 5 and 6 peaks respectively.

3.1.2. DNS

Two-dimensional spatial direct numerical simulations were performed to investigate the vortical structures and sound fields after the development of A1, S1 and S2 modes for Re=1000. In these simulations we used antisymmetric and/or symmetric disturbances with broadband noise to perturb the normal velocity at the inlet. Simulations with three initial conditions were carried out. In Case 1(A1), Mc=0.38 and we used antisymmetric and symmetric disturbances. In Case 1(S1), Mc=0.38 and we used only symmetric disturbances. In Case 2, Mc=1.51 and we used antisymmetric and symmetric disturbances. (Note that in Case 1(S1), only symmetrical disturbance was used because A1 mode grows faster than S1 mode.)

The vorticity and sound fields are shown in Figs. 4(a) and 4(b) respectively. The contour increments are the same. In Case 1(A1), the vortical field becomes asymmetric with regard to jet centerline, since the antisymmetric mode is dominant. In Case 1(S1), the vorticity field becomes symmetrical due to the growth of the S1 mode, because it was forced only with the symmetrical disturbance. In Case 2, the vorticity field becomes symmetric with regard to jet centerline, since the symmetric mode is dominant and its growth rate is larger than the antisymmetric one. In Case 1(A1) and Case 1(S1), there are pairings of the vortices, but in Case 2, there are no pairings in this computational region. From Fig.4(b), we can see the generation of acoustic waves in Case 1(A1) and Case 1(S1), however the dilatation field of the Case 1(S1) is stronger than the Case 1(A1). In Case 2, acoustic waves can't be seen clearly. The difference of these acoustic fields is explained by vortex pairing, present in Case 1 and absent in Case 2. This absence can be explained by the specified subharmonic modes. In Fig.5, the comparison of the sub-harmonic modes growth rates shows that S1 is unstable at low wave numbers, however S2 is not unstable. From this fact, we conjecture that no pairing of the vortices in the flow fields is due to less development of S2 subharmonic mode. Therefore, the generation of the acoustic waves is very weak. Unfortunately, it could not be confirmed here, but we believe that the effect of A1 mode could appear in the far downstream.

3.2. 3-D Results

3.2.1. linear stability

Fig.6 is the result of linear stability analysis for Re=1000. Varying the Mach number affects the dominant mode. For Mc less than 0.8, the dominant mode is 2-D A1. For Mach number larger than 0.8 and less than 1.5 the most unstable mode is 3-D A1, and near Mc=1.13, the dominant 2-D mode changes from A1 to S2. For Mc over 1.5, the dominant mode is 2-D S2.

3.2.2. DNS

Three-dimensional temporal direct numerical simulations were performed to investigate flow structures due to 2-D symmetric (2-D S2) and 3-D antisymmetric (3-D A1) modes. The mean profile was forced with the most unstable 2-D and 3-D modes. The amplitude of the disturbances was about 1% of the jet velocity. The simulations with two initial conditions were carried out. In Case 1, the amplitudes of the 2-D and 3-D disturbances ($\theta = \pm 51^\circ$) were 1% and 0.5 % of the jet velocity. In Case 2, the amplitudes of the 2-D and 3-D disturbances ($\theta = \pm 51^\circ$) were 1% of the jet velocity.

Fig.7 shows the time development of u fluctuation. In this Mach number, linear growth rate of 3-D A1 mode is larger than 2-D S2 one, however in Case 1 the energy growth of 3-D modes is surpressed by grown up 2-D mode. In Case 2, the energy of 3-D A1 mode became close to the 2-D S2 one and this is due to the increase of initial 3-D disturbances.

Fig.8 shows the developed structures of 3-D flow motions from the prescribed initial condition for the Case 1 at t=64. Top and bottom figures show the pressure and dilatation fields respectively. In the top figure, the maximum value of pressure exists around the jet center plane, but no significant three-dimensional structures were found. As for the acoustic filed, the very strong dilatation is formed around the jet center plane but the acoustic filed was weak in the far field. In Case 2, pressure fields at t=64 (shown in Fig.9) exhibit the signficant three-dimensional structure. As for the acoustic filed, although three-dimensionality starts to appear, the main features hold as in Case 1.

4. Summary

Linear stability analyses and direct numerical simulations of Supersonic Plane Jet were performed. From the linear stability study, we found that the dominant mode depends upon the Mach numbers. Two-dimensional spatial DNS show difficulty of pairing of the vortices in a flow where S2 is dominant. Therefore, the generation of the acoustic waves is very weak. From the three-dimensional temporal DNS, in Mc=1.13, it was confirmed that the structure of the flow field depended on the initial conditions, because the linear growth rates of the 2-D S2 and 3-D A1 modes were comparatively similar. Nevertheless more simulations are needed to investigate the effects of other modes.

Acknowledgments

This work was supported with a grant-in-aid (No.12004713) from the Japanese Ministry of Education and Culture. Some of the simulations were executed at the Information Technology Center of the University of Tokyo.

References

1)Lele, S. K., and Moin, P., *AIAA/CEAS.*,**98-2291** (1998) ,1-12.

2) Colonius, T., Lele, S. K. and Moin, P., *J. Fluid Mech.* **330** (1997) 375-409.

3)Mitchell, B. E., Lele, S. K. and Moin, P., *J. Fluid Mech.* , **383** (1999) 113-142.

4)Lele, S. K., *J. Comput. Phys.*, **103** (1992)16-42.

5)Kudryavtsev, A. and Khotyanovsky, D., *Advances in Turbulence, Proc. ETC8*, (2000) 161-164.

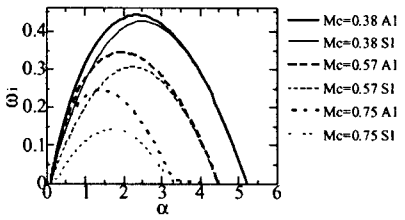

Figure 1. Effect of Mach number on the growth rate of 2-D waves for Mc=0.38-0.75 and Re=1000.

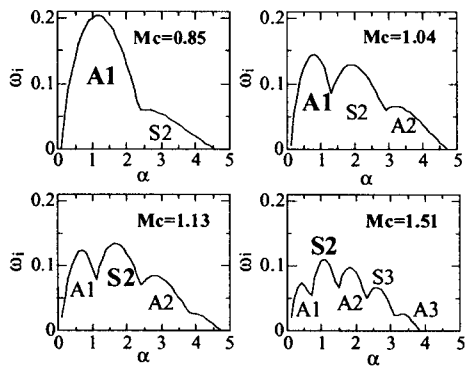

Figure 2. Effect of Mach number on the growth rate of 2-D waves for Mc=0.85-1.51 and Re=1000.

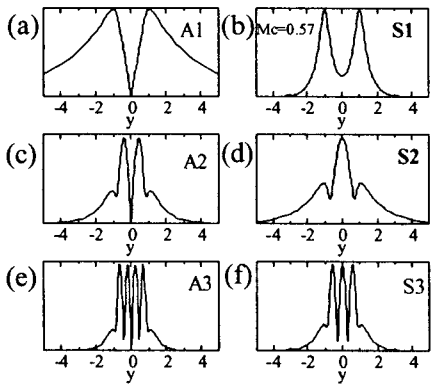

Figure 3. Eigenfunctions of pressure; (a)A1 mode, (b)S1 mode, (c)A2 mode, (d)S2 mode,(e)A3 mode, (f)S3 mode for Mc=1.51 and Re=1000.

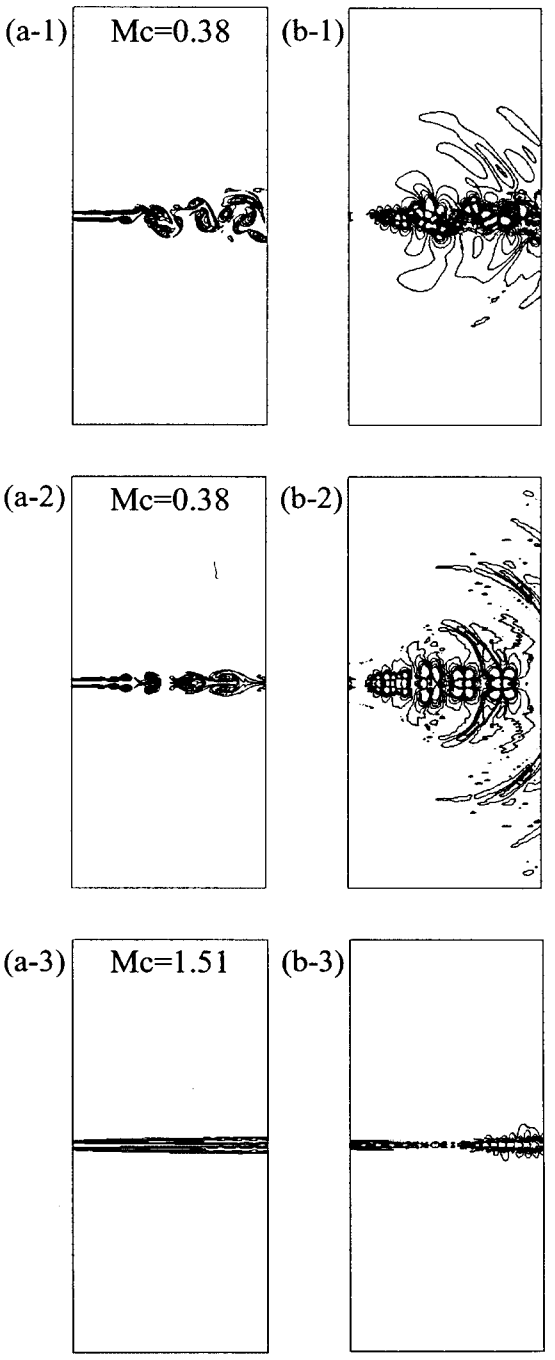

Figure 4. Contour plots of (a) vorticity and (b) dilatation; (a-1) (b-1) Case 1 (A1) (Mc=0.38), (a-2) (b-2) Case 1 (S1) (Mc=0.38) and (a-3) (b-3) Case2 (S2) (Mc=1.51) for Re=1000.

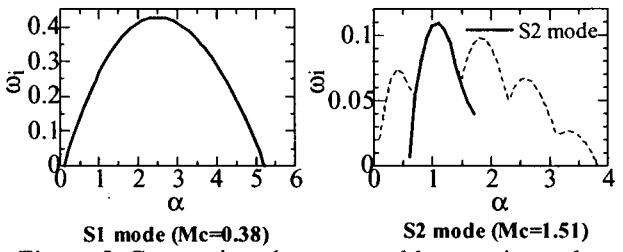

Figure 5. Comparison between subharmonic modes of S1 and S2.

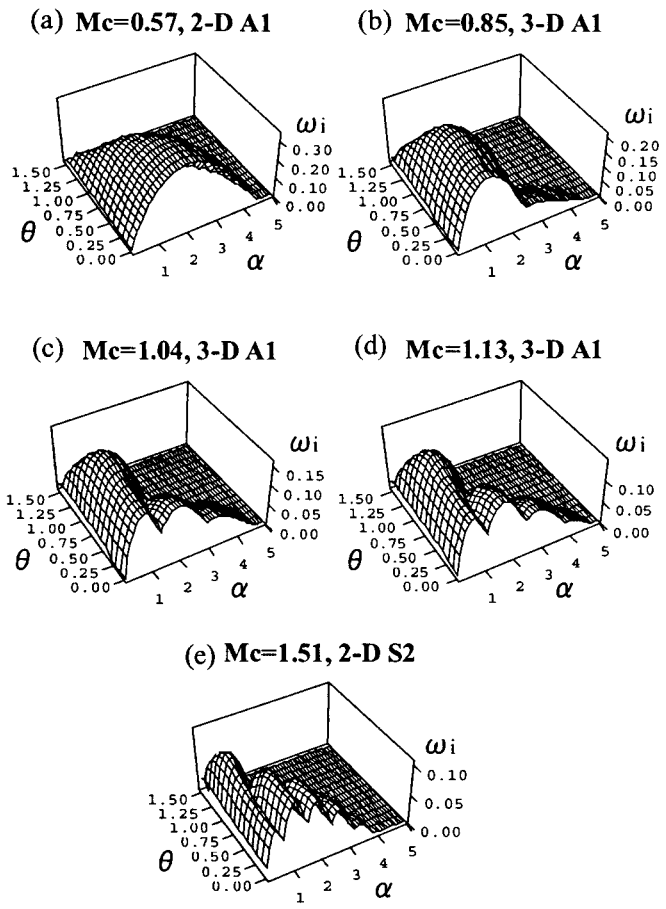

Figure 6. Effect of θ on the growth rate of 3-D waves; (a)Mc=0.57, (b)Mc=0.85, (c)Mc=1.04, (d)Mc=1.13, (e)Mc=1.51 for Re=1000.

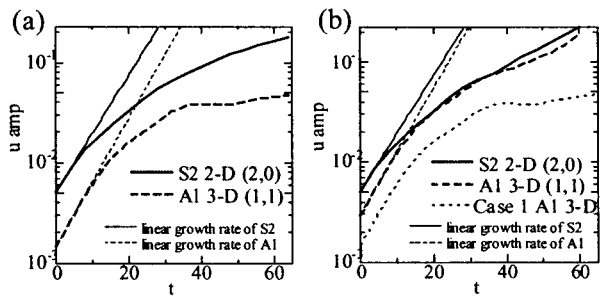

Figure 7. Evolution of u fluctuation magnitude for S2 2-D mode(2,0) and A1 3-D mode (1,1); (a) Case 1, (b) Case 2 for Mc=1.13 and Re=1000.

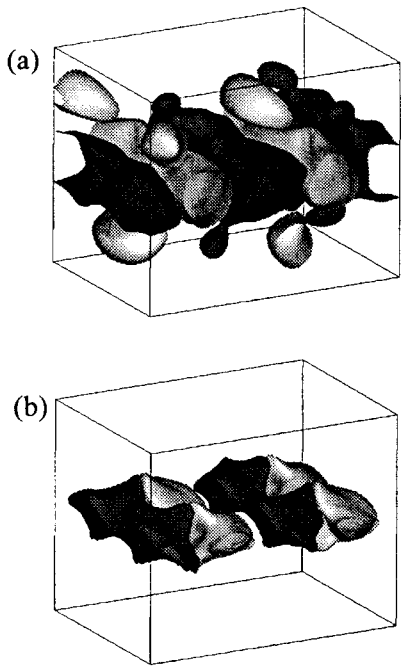

Figure 8. Iso-surfaces of (a) pressure; (b) dilatation at t=64 for Case1, Mc=1.13 and Re=1000.

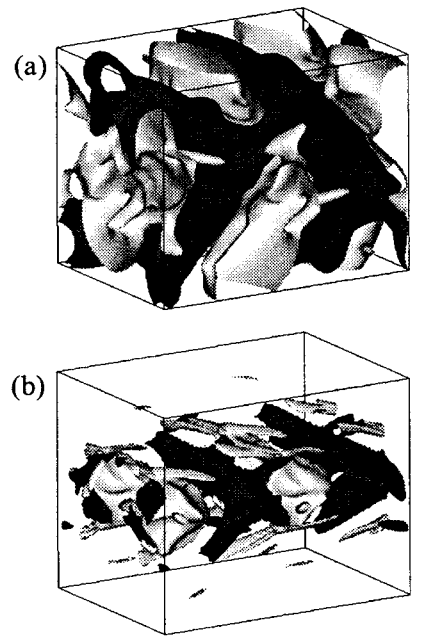

Figure 9. Iso-surfaces of (a) pressure; (b) dilatation at t=64 for Case2, Mc=1.13 and Re=1000.